

Grounding DINO: Marrying DINO with Grounded Pre-Training for Open-Set Object Detection

Shilong Liu^{1,2*}, Zhaoyang Zeng², Tianhe Ren², Feng Li^{2, 3}, Hao Zhang^{2, 3}, Jie Yang^{2, 4}, Chunyuan Li⁵, Jianwei Yang⁵, Hang Su¹, Jun Zhu^{1†}, Lei Zhang^{2†}

¹ Dept. of Comp. Sci. and Tech., BNRist Center, State Key Lab for Intell. Tech. & Sys., Institute for AI, Tsinghua-Bosch Joint Center for ML, Tsinghua University

² International Digital Economy Academy (IDEA)

³ The Hong Kong University of Science and Technology

⁴ The Chinese University of Hong Kong (Shenzhen) ⁵ Microsoft Research, Redmond

liusl20@mails.tsinghua.edu.cn {zengzhaoyang, rentianhe}@idea.edu.cn {fliay, hzhangcx}@connect.ust.hk jieyang5@link.cuhk.edu.cn
 {chunyl, jianwei.yang}@microsoft.com {suhangss, dcszj}@mail.tsinghua.edu.cn leizhang@idea.edu.cn

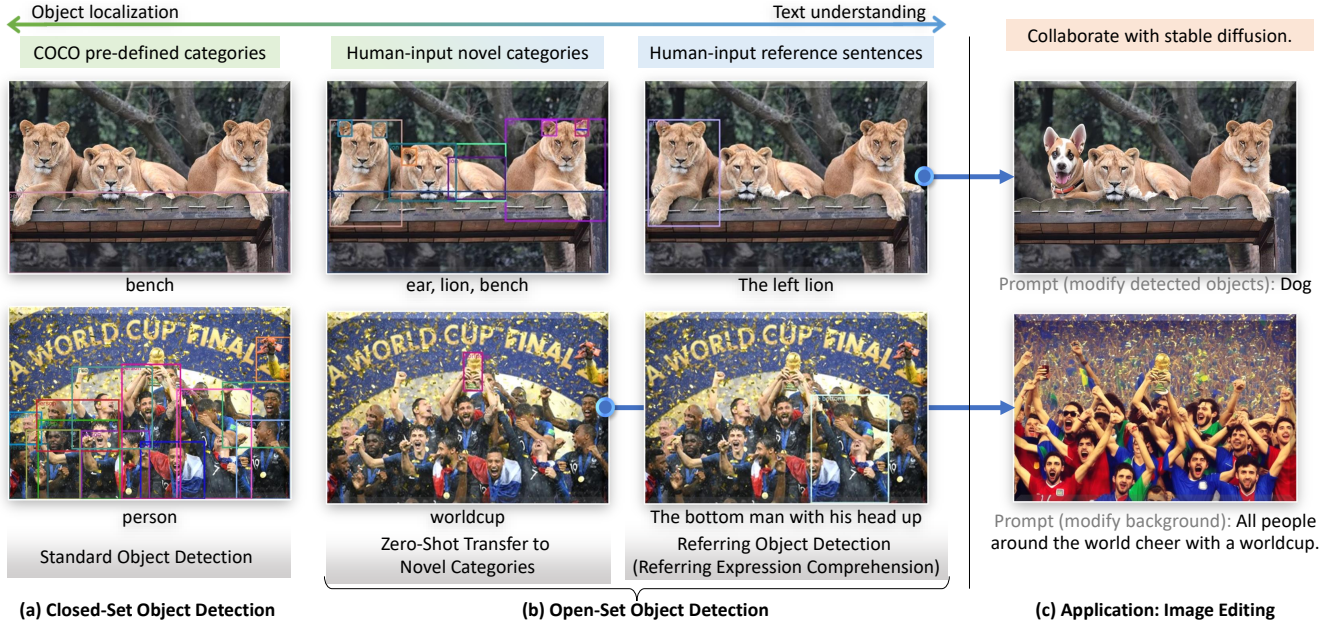


Figure 1. (a) Closed-set object detection requires models to detect objects of pre-defined categories. (b) Previous work zero-shot transfer models to novel categories for model generalization. We propose to add Referring expression comprehension (REC) as another evaluation for model generalizations on novel objects with attributes. (c) We present an image editing application by combining Grounding DINO and Stable Diffusion [42]. Best view in colors.

Abstract

In this paper, we present an open-set object detector, called Grounding DINO, by marrying Transformer-based detector DINO with grounded pre-training, which can detect arbitrary objects with human inputs such as category

* This work was done when Shilong Liu, Feng Li, Hao Zhang, and Jie Yang were interns at IDEA. † Corresponding authors.

names or referring expressions. The key solution of open-set object detection is introducing language to a closed-set detector for open-set concept generalization. To effectively fuse language and vision modalities, we conceptually divide a closed-set detector into three phases and propose a tight fusion solution, which includes a feature enhancer, a language-guided query selection, and a cross-modality

decoder for cross-modality fusion. While previous works mainly evaluate open-set object detection on novel categories, we propose to also perform evaluations on referring expression comprehension for objects specified with attributes. Grounding DINO performs remarkably well on all three settings, including benchmarks on COCO, LVIS, ODinW, and RefCOCO/+g. Grounding DINO achieves a 52.5 AP on the COCO detection zero-shot transfer benchmark, i.e., without any training data from COCO. After fine-tuning with COCO data, Grounding DINO reaches 63.0 AP. It sets a new record on the ODinW zero-shot benchmark with a mean 26.1 AP. Code will be available at <https://github.com/IDEA-Research/GroundingDINO>.

1. Introduction

Understanding novel concepts is a fundamental capability of visual intelligence. In this work, we aim to develop a strong system to detect arbitrary objects specified by human language inputs, which we name as *open-set object detection*¹. The task has wide applications for its great potential as a generic object detector. For example, we can cooperate it with generative models for image editing (as shown in Fig. 1 (b)).

The key to open-set detection is introducing language for unseen object generalization [1, 7, 26]. For example, GLIP [26] reformulates object detection as a phrase grounding task and introduces contrastive training between object regions and language phrases. It shows a great flexibility for heterogeneous datasets and remarkable performance on both closed-set and open-set detection. Despite its impressive results, GLIP’s performance can be constrained since it is designed based on a traditional one-stage detector Dynamic Head [5]. As open-set and closed-set detection are closely related, we believe a stronger closed-set object detector can result in an even better open-set detector.

Motivated by the encouraging progress of Transformer-based detectors [24, 25, 31, 58], in this work, we propose to build a strong open-set detector based on DINO [58], which not only offers the state-of-the-art object detection performance, but also allows us to integrate multi-level text information into its algorithm by grounded pre-training. We name the model as **Grounding DINO**. Grounding DINO has several advantages over GLIP. First, its Transformer-based architecture is similar to language models, making it easier to process both image and language data. For example, as all the image and language branches are built with Transformers, we can easily fuse cross-modality features in its whole pipeline. Second, Transformer-based detectors have demonstrated a superior capability of leveraging large-

¹We view the terms *open-set object detection*, *open-world object detection*, and *open-vocabulary object detection* the same task in this paper. To avoid confusion, we always use *open-set object detection* in our paper.

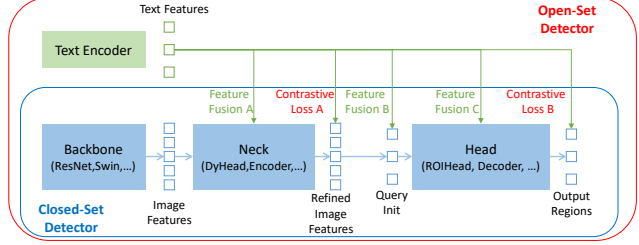


Figure 2. Existing approaches to extending closed-set detectors to open-set scenarios. Note that some closed-set detectors can have only partial phases of the figure.

scale datasets. Lastly, as a DETR-like model, DINO can be optimized end-to-end without using any hard-crafted modules such as NMS (Non-Maximum Suppression), which greatly simplifies the overall grounding model design.

Most existing open-set detectors are developed by extending closed-set detectors to open-set scenarios with language information. As shown in Fig. 2, a closed-set detector typically has three important modules, a backbone for feature extraction, a neck for feature enhancement, and a head for region refinement (or box prediction). A closed-set detector can be generalized to detect novel objects by learning language-aware region embeddings so that each region can be classified into novel categories in a language-aware semantic space. The key to achieving this goal is using contrastive loss between region outputs and language features at the neck and/or head outputs. To help a model align cross-modality information, some work tried to fuse features before the final loss stage. Fig. 2 shows that feature fusion can be performed in three phases: neck (phase A), query initialization (phase B), and head (phase C). For example, GLIP [26] performs early fusion in the neck module (phase A), and OV-DETR [56] uses language-aware queries as head inputs (phase B).

We argue that more feature fusion in the pipeline enables the model to perform better. It is worth noting that retrieval tasks prefer a CLIP-like two-tower architecture which only performs multi-modality feature comparison at the end for efficiency. However, for open-set detection, the model is normally given both an image and a text input that specifies the target object categories or a specific object. In such a case, a tight (and early) fusion model is more preferred for a better performance [1, 26] as both image and text are available at beginning. Although conceptually simple, it is hard for previous work to perform feature fusion in all three phases. The design of classical detectors like Faster RCNN makes it hard to interact with language information in most blocks. Unlike classical detectors, the Transformer-based detector DINO has a consistent structure with language blocks. The layer-by-layer design enables it to interact with language information easily. Under this principle, we design three feature fusion approaches in the neck,

query initialization, and head phases. More specifically, we design a feature enhancer by stacking self-attention, text-to-image cross-attention, and image-to-text cross-attention as the neck module. We then develop a language-guided query selection method to initialize queries for head. We also design a cross-modality decoder for the head phase with image and text cross-attention layers to boost query representations. The three fusion phases effectively help the model achieve better performance on existing benchmarks, which will be shown in Sec. 4.4.

Although significant improvements have been achieved in multi-modal learning, most existing open-set detection work evaluates their models on objects of novel categories, as shown in the left column of Fig. 1 (b). We argue that another important scenario, where objects are described with attributes, should also be considered. In the literature, the task is named Referring Expression Comprehension (REC) [30, 34]². We present some examples of REC in the right column of Fig. 1 (b). It is a closely related field but tends to be overlooked in previous open-set detection work. In this work, we extend open-set detection to support REC and also evaluate its performance on REC datasets.

We conduct experiments on all three settings, including closed-set detection, open-set detection, and referring object detection, to comprehensively evaluate open-set detection performance. Grounding DINO outperforms competitors by a large margin. For example, Grounding DINO reaches a 52.5 AP on COCO minival without any COCO training data. It also establishes a new state of the art on the ODinW [23] zero-shot benchmark with a 26.1 mean AP.

The contributions of this paper are summarized as follows:

1. We propose Grounding DINO, which extends a closed-set detector DINO by performing vision-language modality fusion at multiple phases, including a feature enhancer, a language-guided query selection module, and a cross-modality decoder. Such a deep fusion strategy effectively improves open-set object detection.
2. We propose to extend the evaluation of open-set object detection to REC datasets. It helps evaluate the performance of the model with freeform text inputs.
3. The experiments on COCO, LVIS, ODinW, and RefCOCO+/g datasets demonstrate the effectiveness of Grounding DINO on open-set object detection tasks.

2. Related Work

Detection Transformers. Grounding DINO is built upon the DETR-like model DINO [58], which is an end-to-end Transformer-based detector. DETR was first proposed in [2] and then has been improved from many direc-

²We use the term *Referring Expression Comprehension (REC)* and *Referring (Object) Detection* exchangeable in this paper.

tions [4, 5, 12, 17, 33, 50, 64] in the past few years. DAB-DETR [31] introduces anchor boxes as DETR queries for more accurate box prediction. DN-DETR [24] proposes a query denoising approach to stabilizing the bipartite matching. DINO [58] further develops several techniques including contrastive de-noising and set a new record on the COCO object detection benchmark. However, such detectors mainly focus on closed-set detection and are difficult to generalize to novel classes because of the limited pre-defined categories.

Open-Set Object Detection. Open-set object detection is trained using existing bounding box annotations and aims at detecting arbitrary classes with the help of language generalization. OV-DETR [57] uses image and text embedding encoded by a CLIP model as queries to decode the category-specified boxes in the DETR framework [2]. ViLD [13] distills knowledge from a CLIP teacher model into a R-CNN-like detector so that the learned region embeddings contain the semantics of language. GLIP [11] formulates object detection as a grounding problem and leverages additional grounding data to help learn aligned semantics at phrase and region levels. It shows that such a formulation can even achieve stronger performance on fully-supervised detection benchmarks. DetCLIP [53] involves large-scale image captioning datasets and uses the generated pseudo labels to expand the knowledge database. The generated pseudo labels effectively help extend the generalization ability of the detectors.

However, previous works only fuse multi-modal information in partial phases, which may lead to sub-optimal language generalization ability. For example, GLIP only considers fusion in the feature enhancement (phase A) and OV-DETR only injects language information at the decoder inputs (phase B). Moreover, the REC task is normally overlooked in evaluation, which is an important scenario for open-set detection. We compare our model with other open-set methods in Table 1.

3. Grounding DINO

Grounding DINO outputs multiple pairs of object boxes and noun phrases for a given (Image, Text) pair. For example, as shown in Fig. 3, the model locates a cat and a table from the input image and extracts word `cat` and `table` from the input text as corresponding labels. Both object detection and REC tasks can be aligned with the pipeline. Following GLIP [26], we concatenate all category names as input texts for object detection tasks. REC requires a bounding box for each text input. We use the output object with the largest scores as the output for the REC task.

Grounding DINO is a dual-encoder-single-decoder architecture. It contains an image backbone for image feature extraction, a text backbone for text feature extraction, a fea-

Model	Base Detector	Model Design		Text Prompt	Represent. Level (Sec. 3.4)	Closed-Set Settings	Zero-Shot Transfer			Referring Detection
		Fusion Phases (Fig. 2)	use CLIP				COCO	LVIS	ODinW	
ViLD [13]	Mask R-CNN [15]	-	✓	sentence		✓	partial label	partial label		
RegionCLIP [62]	Faster RCNN [39]	-	✓	sentence		✓	partial label	partial label		
FindIt [21]	Faster RCNN [39]	A		sentence		✓	partial label	partial label		
MDETR [18]	DETR [2]	A,C		word		✓	fine-tune	zero-shot		
DQ-DETR [46]	DETR [2]	A,C		word		✓	zero-shot	zero-shot		
GLIP [26]	DyHead [5]	A		word		✓	zero-shot	zero-shot		
GLIPv2 [59]	DyHead [5]	A		word		✓	zero-shot	zero-shot		
OV-DETR [56]	Deformable DETR [64]	B	✓	sentence		✓	partial label	partial label		
OWL-ViT [35]	-	-	✓	sentence		✓	partial label	partial label		
DetCLIP [53]	ATSS [60]	-	✓	sentence		✓	partial label	partial label		
OmDet [61]	Sparse R-CNN [47]	C	✓	sentence		✓	partial label	partial label		
Grounding DINO (Ours)	DINO [58]	A,B,C		sub-sentence		✓	zero-shot	zero-shot	zero-shot	zero-shot

Table 1. A comparison of previous open-set object detectors. Our summarization is based on the experiments in their paper, but not the ability to extend their models to other tasks. It is worth noting that some related works may not (only) be designed for the open-set object detection initially, like MDETR [18] and GLIPv2 [59], but we list them here for a comprehensive comparison with existing work. We use the term ‘‘partial label’’ for the settings, where models are trained on partial data (e.g. base categories) and evaluated on other cases.

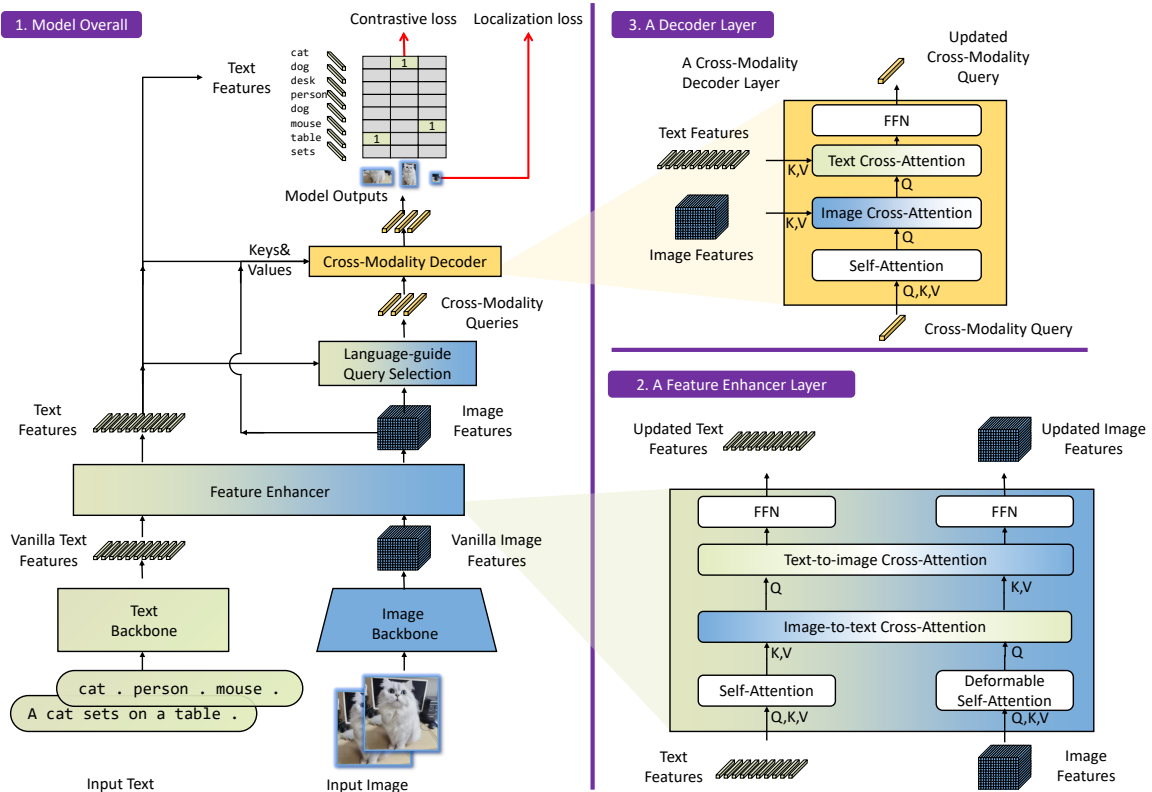


Figure 3. The framework of Grounding DINO. We present the overall framework, a feature enhancer layer, and a decoder layer in block 1, block 2, and block 3, respectively.

ture enhancer for image and text feature fusion (Sec. 3.1), a language-guided query selection module for query initialization (Sec. 3.2), and a cross-modality decoder for box refinement (Sec. 3.3). The overall framework is available in Fig. 3.

For each (Image, Text) pair, we first extract vanilla image features and vanilla text features using an image backbone and a text backbone, respectively. The two vanilla features are fed into a feature enhancer module for cross-modality feature fusion. After obtaining cross-modality text

and image features, we use a language-guided query selection module to select cross-modality queries from image features. Like the object queries in most DETR-like models, these cross-modality queries will be fed into a cross-modality decoder to probe desired features from the two modal features and update themselves. The output queries of the last decoder layer will be used to predict object boxes and extract corresponding phrases.

3.1. Feature Extraction and Enhancer

Given an (Image, Text) pair, we extract multi-scale image features with an image backbone like Swin Transformer [32], and text features with a text backbone like BERT [8]. Following previous DETR-like detectors [58, 64], multi-scale features are extracted from the outputs of different blocks. After extracting vanilla image and text features, we fed them into a feature enhancer for cross-modality feature fusion. The feature enhancer includes multiple feature enhancer layers. We illustrate a feature enhancer layer in Fig. 3 block 2. We leverage the Deformable self-attention to enhance image features and the vanilla self-attention for text feature enhancers. Inspired by GLIP [26], we add an image-to-text cross-attention and a text-to-image cross-attention for feature fusion. These modules help align features of different modalities.

3.2. Language-Guided Query Selection

Grounding DINO aims to detect objects from an image specified by an input text. To effectively leverage the input text to guide object detection, we design a language-guided query selection module to select features that are more relevant to the input text as decoder queries. We present the query selection process in Algorithm 1 in PyTorch style. The variables `image_features` and `text_features` are used for image and text features, respectively. `num_query` is the number of queries in the decoder, which is set to 900 in our implementation. We use `bs` and `ndim` for batch size and feature dimension in the pseudo-code. `num_img_tokens` and `num_text_tokens` are used for the number of image and text tokens, respectively.

The language-guided query selection module outputs `num_query` indices. We can extract features based on the selected indices to initialize queries. Following DINO [58], we use mixed query selection to initialize decoder queries. Each decoder query contains two parts: content part and positional part [33], respectively. We formulate the positional part as dynamic anchor boxes [31], which are initialized with encoder outputs. The other part, the content queries, are set to be learnable during training.

3.3. Cross-Modality Decoder

We develop a cross-modality decoder to combine image and text modality features, as shown in Fig. 3 block 3. Each cross-modality query is fed into a self-attention layer, an image cross-attention layer to combine image features, a text cross-attention layer to combine text features, and an FFN layer in each cross-modality decoder layer. Each decoder layer has an extra text cross-attention layer compared with the DINO decoder layer, as we need to inject text information into queries for better modality alignment.

Algorithm 1 Language-guided query selection.

```

"""
Input:
image_features: (bs, num_img_tokens, ndim)
text_features: (bs, num_text_tokens, ndim)
num_query: int.

Output:
topk_proposals_idx: (bs, num_query)
"""

logits = torch.einsum("bic,btc->bit",
                      image_features, text_features)
# bs, num_img_tokens, num_text_tokens

logits_per_img_feat = logits.max(-1)[0]
# bs, num_img_tokens

topk_proposals_idx = torch.topk(
    logits_per_image_feature,
    num_query, dim=1)[1]
# bs, num_query

```

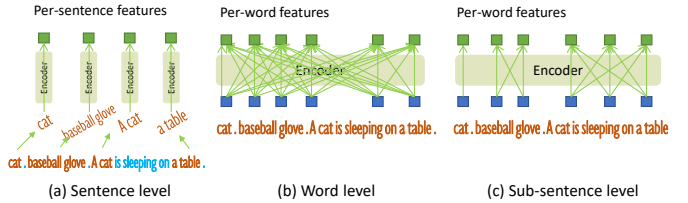


Figure 4. Comparisons of text representations.

3.4. Sub-Sentence Level Text Feature

Two kinds of text prompts are explored in previous works, which we named as sentence level representation and word level representation, as shown in Fig. 4. Sentence level representation [35, 53] encodes a whole sentence to one feature. If some sentences in phrase grounding data have multiple phrases, it extracts these phrases and discards other words. In this way, it removes the influence between words while losing fine-grained information in sentences. Word level representation [11, 18] enables encoding multiple category names with one forward but introduces unnecessary dependencies among categories, especially when the input text is a concatenation of multiple category names in an arbitrary order. As shown in Fig. 4 (b), some unrelated words interact during attention. To avoid unwanted word interactions, we introduce attention masks to block attentions among unrelated category names, named “sub-sentence” level representation. It eliminates the influence between different category names while keeping per-word features for fine-grained understanding.

3.5. Loss Function

Following previous DETR-like works [2, 24, 31, 33, 58, 64], we use the L1 loss and the GIOU [41] loss for bounding box regressions. We follow GLIP [26] and use contrastive loss between predicted objects and language tokens

for classification. Specifically, we dot product each query with text features to predict logits for each text token and then compute focal loss [28] for each logit. Box regression and classification costs are first used for bipartite matching between predictions and ground truths. We then calculate final losses between ground truths and matched predictions with the same loss components. Following DETR-like models, we add auxiliary loss after each decoder layer and after the encoder outputs.

4. Experiments

4.1. Setup

We conduct extensive experiments on three settings: a closed-set setting on the COCO detection benchmark (Sec. C.1), an open-set setting on zero-shot COCO, LVIS, and ODinW (Sec. 4.2), and a referring detection setting on RefCOCO/+/g (Sec. 4.3). Ablations are then conducted to show the effectiveness of our model design (Sec. 4.4). We also explore a way to transfer a well-trained DINO to the open-set scenario by training a few plug-in modules in Sec. 4.5. The test of our model efficiency is presented in Sec. I.

Implementation Details We trained two model variants, Grounding-DINO-T with Swin-T [32], and Grounding-DINO-L with Swin-L [32] as an image backbone, respectively. We leveraged BERT-base [8] from Hugging Face [51] as text backbones. As we focus more on the model performance on novel classes, we list zero-shot transfer and referring detection results in the main text. More implementation details are available in the Appendix Sec. A.

4.2. Zero-Shot Transfer of Grounding DINO

In this setting, we pre-train models on large-scale datasets and directly evaluate models on new datasets. We also list some fine-tuned results for a more thorough comparison of our model with prior works.

COCO Benchmark We compare Grounding DINO with GLIP and DINO in Table 2. We pre-train models on large-scale datasets and directly evaluate our model on the COCO benchmark. As the O365 dataset [44] has (nearly³) covered all categories in COCO, we evaluate an O365 pre-trained DINO on COCO as a zero-shot baseline. The result shows that DINO performs better on the COCO zero-shot transfer than DyHead. Grounding DINO outperforms all previous models on the zero-shot transfer setting, with +0.5AP and +1.8AP compared with DINO and GLIP under the same setting. Grounding data is still helpful for Grounding DINO, introducing more than 1AP (48.1 vs. 46.7) on the zero-shot transfer setting. With stronger backbones and larger data, Grounding DINO sets a new record of 52.5 AP

³It is not an exact mapping between O365 and COCO categories. We made some approximations during evaluation.

on the COCO object detection benchmark without seeing any COCO images during training. Grounding DINO obtains a 62.6 AP on COCO minival, outperforming DINO’s 62.5 AP. When enlarging the input images by 1.5 \times , the benefits reduce. We suspect that the text branch enlarges the gap between models with different input images. Even though, Grounding DINO gets an impressive 63.0 AP on COCO test-dev with fine-tuning on the COCO dataset (See the number in brackets of Table 2).

LVIS Benchmark LVIS [14] is a dataset for long-tail objects. It contains more than 1000 categories for evaluation. We use LVIS as a downstream task to test the zero-shot abilities of our model. We use GLIP as baselines for our models. The results are shown in Table 3. Grounding DINO outperforms GLIP under the same settings. We found two interesting phenomena in the results. First, Grounding DINO works better than common objects than GLIP, but worse on rare categories. We suspect that the 900 query design limits the ability for long-tailed objects. By contrast, the one-stage detector uses all proposals in the feature map for comparisons. The other phenomenon is that Grounding DINO has larger gains with more data than GLIP. For example, Grounding DINO introduces +1.8 AP gains with the caption data Cap4M, whereas GLIP has only +1.1 AP. We believe that Grounding DINO has a better scalability compared with GLIP. A larger-scale training will be left as our future work.

ODinW Benchmark ODinW (Object Detection in the Wild) [23] is a more challenging benchmark to test model performance under real-world scenarios. It collects more than 35 datasets for evaluation. We report three settings, zero-shot, few-shot, and full-shot results in Table 4. Grounding DINO performs well on this benchmark. With only O365 and GoldG for pre-train, Grounding-DINO-T outperforms DINO on few-shot and full-shot settings. Impressively, Grounding DINO with a Swin-T backbone outperforms DINO with Swin-L on the full-shot setting. Grounding DINO outperforms GLIP under the same backbone for the zero-shot setting, comparable with GLIPv2 [59] without any new techniques like masked training. The results show the superiority of our proposed models. Grounding-DINO-L set a new record on ODinW zero-shot with a 26.1 AP, even outperforming the giant Florence models [55]. The results show the generalization and scalability of Grounding DINO.

4.3. Referring Object Detection Settings

We further explore our models’ performances on the REC task. We leverage GLIP [26] as our baseline. We

Model	Backbone	Pre-Training Data	Zero-Shot 2017val	Fine-Tuning 2017val/test-dev
Faster R-CNN	RN50-FPN	-	-	40.2 / -
Faster R-CNN	RN101-FPN	-	-	42.0 / -
DyHead-T [5]	Swin-T	-	-	49.7 / -
DyHead-L [5]	Swin-L	-	-	58.4 / 58.7
DyHead-L [5]	Swin-L	O365,ImageNet21K	-	60.3 / 60.6
SoftTeacher [52]	Swin-L	O365,SS-COCO	-	60.7 / 61.3
DINO(Swin-L) [58]	Swin-L	O365	-	62.5 / -
DyHead-T† [5]	Swin-T	O365	43.6	53.3 / -
GLIP-T (B) [26]	Swin-T	O365	44.9	53.8 / -
GLIP-T (C) [26]	Swin-T	O365,GoldG	46.7	55.1 / -
GLIP-L [26]	Swin-L	FourODs,GoldG,Cap24M	49.8	60.8 / 61.0
DINO(Swin-T)† [58]	Swin-T	O365	46.2	56.9 / -
Grounding-DINO-T (Ours)	Swin-T	O365	46.7	56.9 / -
Grounding-DINO-T (Ours)	Swin-T	O365,GoldG	48.1	57.1 / -
Grounding-DINO-T (Ours)	Swin-T	O365,GoldG,Cap4M	48.4	57.2 / -
Grounding-DINO-L (Ours)	Swin-L	O365,OI [19],GoldG	52.5	62.6 / 62.7 (63.0 / 63.0)*
Grounding-DINO-L (Ours)	Swin-L	O365,OI,GoldG,Cap4M,COCO,RefC	60.7	62.6 / -

Table 2. Zero-shot domain transfer and fine-tuning on COCO. * The results in brackets are trained with $1.5 \times$ image sizes, i.e., with a maximum image size of 2000. †The models map a subset of O365 categories to COCO for zero-shot evaluations.

Model	Backbone	Pre-Training Data	Minival [18]		
			AP	AP _r	AP _c /AP _f
MDETR [18]*	RN101	GoldG,RefC	24.2	20.9/24.9/24.3	
Mask R-CNN [18]*	RN101	-	33.3	26.3/34.0/33.9	
GLIP-T (C)	Swin-T	O365,GoldG	24.9	17.7/19.5/31.0	
GLIP-T	Swin-T	O365,GoldG,Cap4M	26.0	20.8/21.4/31.0	
Grounding-DINO-T	Swin-T	O365,GoldG	25.6	14.4/19.6/32.2	
Grounding-DINO-T	Swin-T	O365,GoldG,Cap4M	27.4	18.1/23.3/32.7	
Grounding-DINO-L	Swin-L	O365,OI,GoldG,Cap4M,COCO,RefC	33.9	22.2/30.7/38.8	

Table 3. Zero-shot domain transfer to LVIS. *The models are fine-tuned on the LVIS dataset before evaluation.

evaluate the model performance on RefCOCO/+g directly.⁴ The results are shown in Table 5. Grounding DINO outperforms GLIP under the same setting. Nevertheless, both GLIP and Grounding DINO perform not well without REC data. More training data like caption data or larger models help the final performance, but quite minor. After injecting RefCOCO/+g data into training, Grounding DINO obtains significant gains. The results reveal that most nowadays open-set object detectors need to pay more attention for a more fine-grained detection.

4.4. Ablations

We conduct ablation studies in this section. We propose a tight fusion grounding model for open-set object detection and a sub-sentence level text prompt. To verify the effectiveness of the model design, we remove some fusion blocks for different variants. Results are shown in Table 6. All models are pre-trained on O365 with a Swin-T backbone. The results show that each fusion helps the final per-

formance. Encoder fusion is the most important design. The impact of word-level text prompts the smallest, but helpful as well. The language-guided query selection and text cross-attention present a larger influence on LVIS and COCO, respectively.

4.5. Transfer from DINO to Grounding DINO

Recent work has presented many large-scale image models for detection with DINO architecture⁵. It is computationally expensive to train a Grounding DINO model from scratch. However, the cost can be significantly reduced if we leverage pre-trained DINO weights. Hence, we conduct some experiments to transfer pre-trained DINO to Grounding DINO models. We freeze the modules co-existing in DINO and Grounding DINO and fine-tune the other parameters only. (We compare DINO and Grounding DINO in Sec. E.) The results are available in Table 7.

It shows that we can achieve similar performances with Grounding-DINO-Training only text and fusion blocks using a pre-trained DINO. Interestingly, the DINO-pre-trained Grounding DINO outperforms standard Grounding DINO on LVIS under the same setting. The results show that there might be much room for model training improvement, which will be our future work to explore. With a pre-trained DINO initialization, the model converges faster than Grounding DINO from scratch, as shown in Fig. 5. Notably, we use the results without exponential moving average (EMA) for the curves in Fig. 5, which results in a different final performance that in Table 7. As the model

⁴We used the official released code and checkpoints in <https://github.com/microsoft/GLIP>.

⁵See model instances at <https://github.com/IDEA-Research/detrex>

Model	Language Input	Backbone	Model Size	Pre-Training Data	Test	AP _{average}	AP _{median}
<i>Zero-Shot Setting</i>							
MDETR [18]	✓	ENB5 [48]	169M	GoldG,RefC	10.7	3.0	
OWL-ViT [35]	✓	ViT L/14(CLIP)	>1243M	O365, VG	18.8	9.8	
GLIP-T [26]	✓	Swin-T	232M	O365,GoldG,Cap4M	19.6	5.1	
OmDet [61]	✓	ConvNeXt-B	230M	COCO,O365,LVIS,PhraseCut	19.7	10.8	
GLIPv2-T [59]	✓	Swin-T	232M	O365,GoldG,Cap4M	22.3	8.9	
DetCLIP [53]	✓	Swin-L	267M	O365,GoldG,YFCC1M	24.9	18.3	
Florence [55]	✓	CoSwinH	≈841M	FLD900M,O365,GoldG	25.8	14.3	
Grounding-DINO-T(Ours)	✓	Swin-T	172M	O365,GoldG	20.0	9.5	
Grounding-DINO-T(Ours)	✓	Swin-T	172M	O365,GoldG,Cap4M	22.3	11.9	
Grounding DINO L(Ours)	✓	Swin-L	341M	O365,OI,GoldG,Cap4M,COCO,RefC	26.1	18.4	
<i>Few-Shot Setting</i>							
DyHead-T [5]	✗	Swin-T	≈100M	O365	37.5	36.7	
GLIP-T [26]	✓	Swin-T	232M	O365,GoldG,Cap4M	38.9	33.7	
DINO-Swin-T [58]	✗	Swin-T	49M	O365	41.2	41.1	
OmDet [61]	✓	ConvNeXt-B	230M	COCO,O365,LVIS,PhraseCut	42.4	41.7	
Grounding-DINO-T(Ours)	✓	Swin-T	172M	O365,GoldG	46.4	51.1	
<i>Full-Shot Setting</i>							
GLIP-T [26]	✓	Swin-T	232M	O365,GoldG,Cap4M	62.6	62.1	
DyHead-T [5]	✗	Swin-T	≈100M	O365	63.2	64.9	
DINO-Swin-T [58]	✗	Swin-T	49M	O365	66.7	68.5	
OmDet [61]	✓	ConvNeXt-B	230M	COCO,O365,LVIS,PhraseCut	67.1	71.2	
DINO-Swin-L [58]	✗	Swin-L	218M	O365	68.8	70.7	
Grounding-DINO-T(Ours)	✓	Swin-T	172M	O365,GoldG	70.7	76.2	

Table 4. Results on the ODinW benchmark.

Method	Backbone	Pre-Training Data	Fine-tuning	RefCOCO			RefCOCO+		RefCOCOg	
				val	testA	testB	val	testA	testB	val
MAttNet [54]	R101	None	✓	76.65	81.14	69.99	65.33	71.62	56.02	66.58
VGTR [9]	R101	None	✓	79.20	82.32	73.78	63.91	70.09	56.51	65.73
TransVG [7]	R101	None	✓	81.02	82.72	78.35	64.82	70.70	56.94	68.67
VILLA-L* [10]	R101	CC, SBU, COCO, VG	✓	82.39	87.48	74.84	76.17	81.54	66.84	76.18
RefTR [27]	R101	VG	✓	85.65	88.73	81.16	77.55	82.26	68.99	79.25
MDETR [18]	R101	GoldG,RefC	✓	86.75	89.58	81.41	79.52	84.09	70.62	81.64
DQ-DETR [46]	R101	GoldG,RefC	✓	88.63	91.04	83.51	81.66	86.15	73.21	82.76
GLIP-T(B)	Swin-T	O365,GoldG		49.96	54.69	43.06	49.01	53.44	43.42	65.58
GLIP-T	Swin-T	O365,GoldG,Cap4M		50.42	54.30	43.83	49.50	52.78	44.59	66.09
Grounding-DINO-T (Ours)	Swin-T	O365,GoldG		50.41	57.24	43.21	51.40	57.59	45.81	67.46
Grounding-DINO-T (Ours)	Swin-T	O365,GoldG,RefC		73.98	74.88	59.29	66.81	69.91	56.09	71.06
Grounding-DINO-T (Ours)	Swin-T	O365,GoldG,RefC	✓	89.19	91.86	85.99	81.09	87.40	74.71	84.15
Grounding-DINO-L (Ours)*	Swin-L	O365,OI,GoldG,Cap4M,COCO,RefC	✓	90.56	93.19	88.24	82.75	88.95	75.92	86.13

Table 5. Top-1 accuracy comparison on the referring expression comprehension task. We mark the best results in bold. All models are trained with a ResNet-101 backbone. We use the notations “CC”, “SBU”, “VG”, “OI”, “O365”, and “YFCC” for Conceptual Captions [45], SBU Captions [36], Visual Genome [20], OpenImage [22], Objects365 [63], YFCC100M [49] respectively. The term “RefC” is used for RefCOCO, RefCOCO+, and RefCOCOg three datasets. * There might be a data leak since COCO includes validation images in RefC. But the annotations of the two datasets are different.

#ID	Model	COCO minival		LVIS minival Zero-Shot
		Zero-Shot	Fine-Tune	
0	Grounding DINO (Full Model)	46.7	56.9	16.1
1	w/o encoder fusion	45.8	56.1	13.1
2	static query selection	46.3	56.6	13.6
3	w/o text cross-attention	46.1	56.3	14.3
4	word-level text prompt	46.4	56.6	15.6

Table 6. Ablations for our model. All models are trained on the O365 dataset with a Swin Transformer Tiny backbone.

Model	Pre-Train Data		COCO minival Zero-Shot	LVIS minival Zero-Shot	ODinW Zero-Shot
	DINO Pre-Train	Grounded Fine-Tune			
Grounding-DINO-T (from scratch)	-	O365	46.7	16.2	14.5
Grounding-DINO-T (from pre-trained DINO)	O365	O365,GoldG	48.1	25.6	20.0

Table 7. Transfer pre-trained DINO to Grounding DINO. We freeze shared modules between DINO and Grounding DINO during grounded fine-tuning. All models are trained with a Swin Transformer Tiny backbone.

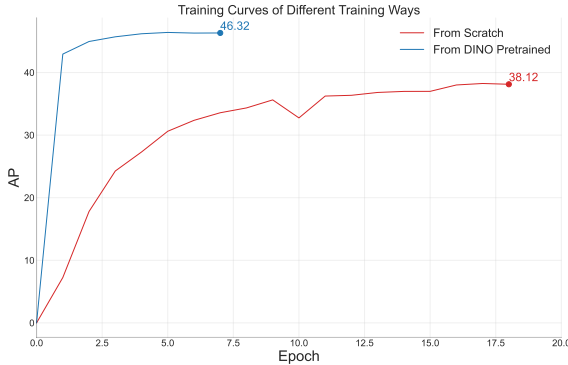


Figure 5. Comparison between two Grounding DINO variants: Training from scratch and transfer from DINO-pretrained models. The models are trained on O365 and evaluated on COCO directly.

trained from scratch need more training time, we only show results of early epochs.

5. Conclusion

We have presented a Grounding DINO model in this paper. Grounding DINO extends DINO to open-set object detection, enabling it to detect arbitrary objects given texts as queries. We review open-set object detector designs and propose a tight fusion approach to better fusing cross-modality information. We propose a sub-sentence level representation to use detection data for text prompts in a more reasonable way. The results show the effectiveness of our model design and fusion approach. Moreover, we extend open-set object detection to REC tasks and perform evaluation accordingly. We show that existing open-set detectors do not work well for REC data without fine-tuning. Hence we call extra attention to REC zero-shot performance in future studies.

Limitations: Although the great performance on open-set object detection setting, Grounding DINO cannot be used for segmentation tasks like GLIPv2. Moreover, our training data is less than the largest GLIP model, which may limit our final performance.

6. Acknowledgement

We thank the authors of GLIP [26]: Liunian Harold Li, Pengchuan Zhang, and Haotian Zhang for their helpful discussions and instructions. We also thank Tiancheng Zhao, the author of OmDet [61], and Jianhua Han, the author of DetCLIP [53], for their response on their model details. We thank He Cao of The Hong Kong University of Science and Technology for his helps on diffusion models.

References

[1] Peter Anderson, Xiaodong He, Chris Buehler, Damien Teney, Mark Johnson, Stephen Gould, and Lei Zhang.

Bottom-up and top-down attention for image captioning and visual question answering. *computer vision and pattern recognition*, 2017. 2

[2] Nicolas Carion, Francisco Massa, Gabriel Synnaeve, Nicolas Usunier, Alexander Kirillov, and Sergey Zagoruyko. End-to-end object detection with transformers. In *European Conference on Computer Vision*, pages 213–229. Springer, 2020. 3, 4, 5, 13

[3] Kai Chen, Jiangmiao Pang, Jiaqi Wang, Yu Xiong, Xiaoxiao Li, Shuyang Sun, Wansen Feng, Ziwei Liu, Jianping Shi, Wanli Ouyang, et al. Hybrid task cascade for instance segmentation. In *Proceedings of the IEEE/CVF Conference on Computer Vision and Pattern Recognition*, pages 4974–4983, 2019. 13

[4] Qiang Chen, Xiaokang Chen, Jian Wang, Haocheng Feng, Junyu Han, Errui Ding, Gang Zeng, and Jingdong Wang. Group detr: Fast detr training with group-wise one-to-many assignment. 2022. 3

[5] Xiyang Dai, Yinpeng Chen, Bin Xiao, Dongdong Chen, Mengchen Liu, Lu Yuan, and Lei Zhang. Dynamic head: Unifying object detection heads with attentions. In *Proceedings of the IEEE/CVF Conference on Computer Vision and Pattern Recognition*, pages 7373–7382, 2021. 2, 3, 4, 7, 8, 13

[6] Xiyang Dai, Yinpeng Chen, Jianwei Yang, Pengchuan Zhang, Lu Yuan, and Lei Zhang. Dynamic detr: End-to-end object detection with dynamic attention. In *Proceedings of the IEEE/CVF International Conference on Computer Vision (ICCV)*, pages 2988–2997, October 2021. 13

[7] Jiajun Deng, Zhengyuan Yang, Tianlang Chen, Wengang Zhou, and Houqiang Li. Transvg: End-to-end visual grounding with transformers. *arXiv: Computer Vision and Pattern Recognition*, 2021. 2, 8

[8] Jacob Devlin, Ming-Wei Chang, Kenton Lee, and Kristina Toutanova. Bert: Pre-training of deep bidirectional transformers for language understanding. *arXiv preprint arXiv:1810.04805*, 2018. 5, 6

[9] Ye Du, Zehua Fu, Qingjie Liu, and Yunhong Wang. Visual grounding with transformers. 2021. 8

[10] Zhe Gan, Yen-Chun Chen, Linjie Li, Chen Zhu, Yu Cheng, and Jingjing Liu. Large-scale adversarial training for vision-and-language representation learning. *neural information processing systems*, 2020. 8

[11] Peng Gao, Shijie Geng, Renrui Zhang, Teli Ma, Rongyao Fang, Yongfeng Zhang, Hongsheng Li, and Yu Qiao. Clip-adapter: Better vision-language models with feature adapters. *arXiv preprint arXiv:2110.04544*, 2021. 3, 5

[12] Peng Gao, Minghang Zheng, Xiaogang Wang, Jifeng Dai, and Hongsheng Li. Fast convergence of detr with spatially modulated co-attention. *arXiv preprint arXiv:2101.07448*, 2021. 3

[13] Xiuye Gu, Tsung-Yi Lin, Weicheng Kuo, and Yin Cui. Open-vocabulary object detection via vision and language knowledge distillation. *Learning*, 2021. 3, 4

[14] Agrim Gupta, Piotr Dollar, and Ross Girshick. Lvis: A dataset for large vocabulary instance segmentation. In *Proceedings of the IEEE/CVF Conference on Computer Vision and Pattern Recognition*, pages 5356–5364, 2019. 6

[15] Kaiming He, Georgia Gkioxari, Piotr Dollár, and Ross Girshick. Mask r-cnn. In *Proceedings of the IEEE international conference on computer vision*, pages 2961–2969, 2017. 4

[16] Kaiming He, Xiangyu Zhang, Shaoqing Ren, and Jian Sun. Deep residual learning for image recognition. In *2016 IEEE Conference on Computer Vision and Pattern Recognition (CVPR)*, pages 770–778, 2016. 12

[17] Ding Jia, Yuhui Yuan, †‡ Haodi He, † Xiaopei Wu, Haojun Yu, Weihong Lin, Lei Sun, Chao Zhang, and Han Hu. Detrs with hybrid matching. 2022. 3

[18] Aishwarya Kamath, Mannat Singh, Yann LeCun, Gabriel Synnaeve, Ishan Misra, and Nicolas Carion. Mdetr-modulated detection for end-to-end multi-modal understanding. In *Proceedings of the IEEE/CVF International Conference on Computer Vision*, pages 1780–1790, 2021. 4, 5, 7, 8, 12

[19] Ivan Krasin, Tom Duerig, Neil Alldrin, Vittorio Ferrari, Sami Abu-El-Haija, Alina Kuznetsova, Hassan Rom, Jasper Uijlings, Stefan Popov, Andreas Veit, et al. Openimages: A public dataset for large-scale multi-label and multi-class image classification. *Dataset available from https://github.com/openimages*, 2(3):18, 2017. 7, 12

[20] Ranjay Krishna, Yuke Zhu, Oliver Groth, Justin Johnson, Kenji Hata, Joshua Kravitz, Stephanie Chen, Yannis Kalantidis, Li-Jia Li, David A. Shamma, Michael S. Bernstein, and Li Fei-Fei. Visual genome: Connecting language and vision using crowdsourced dense image annotations. *International Journal of Computer Vision*, 2017. 8, 12

[21] Weicheng Kuo, Fred Bertsch, Wei Li, AJ Piergiovanni, Mohammad Saffar, and Anelia Angelova. Findit: Generalized localization with natural language queries. 2022. 4

[22] Alina Kuznetsova, Hassan Rom, Neil Alldrin, Jasper Uijlings, Ivan Krasin, Jordi Pont-Tuset, Shahab Kamali, Stefan Popov, Matteo Malloci, Alexander Kolesnikov, Tom Duerig, and Vittorio Ferrari. The open images dataset v4: Unified image classification, object detection, and visual relationship detection at scale. *arXiv: Computer Vision and Pattern Recognition*, 2018. 8

[23] Chunyuan Li, Haotian Liu, Liunian Harold Li, Pengchuan Zhang, Jyoti Aneja, Jianwei Yang, Ping Jin, Yong Jae Lee, Houdong Hu, Zicheng Liu, and Jianfeng Gao. Elevator: A benchmark and toolkit for evaluating language-augmented visual models. 2022. 3, 6

[24] Feng Li, Hao Zhang, Shilong Liu, Jian Guo, Lionel M Ni, and Lei Zhang. Dn-detr: Accelerate detr training by introducing query denoising. In *Proceedings of the IEEE/CVF Conference on Computer Vision and Pattern Recognition*, pages 13619–13627, 2022. 2, 3, 5, 13

[25] Feng Li, Hao Zhang, Huazhe Xu, Shilong Liu, Lei Zhang, Lionel M Ni, and Heung-Yeung Shum. Mask dino: Towards a unified transformer-based framework for object detection and segmentation. 2023. 2

[26] Liunian Harold Li, Pengchuan Zhang, Haotian Zhang, Jianwei Yang, Chunyuan Li, Yiwu Zhong, Lijuan Wang, Lu Yuan, Lei Zhang, Jenq-Neng Hwang, et al. Grounded language-image pre-training. *arXiv preprint arXiv:2112.03857*, 2021. 2, 3, 4, 5, 6, 7, 8, 9, 12, 17

[27] Muchen Li and Leonid Sigal. Referring transformer: A one-step approach to multi-task visual grounding. *arXiv: Computer Vision and Pattern Recognition*, 2021. 8

[28] Tsung-Yi Lin, Priya Goyal, Ross Girshick, Kaiming He, and Piotr Dollár. Focal loss for dense object detection. In *Proceedings of the IEEE international conference on computer vision*, pages 2980–2988, 2017. 6

[29] Tsung-Yi Lin, Michael Maire, Serge Belongie, James Hays, Pietro Perona, Deva Ramanan, Piotr Dollár, and C Lawrence Zitnick. Microsoft coco: Common objects in context. In *European conference on computer vision*, pages 740–755. Springer, 2014. 12

[30] Jingyu Liu, Liang Wang, and Ming-Hsuan Yang. Referring expression generation and comprehension via attributes. *international conference on computer vision*, 2017. 3

[31] Shilong Liu, Feng Li, Hao Zhang, Xiao Yang, Xianbiao Qi, Hang Su, Jun Zhu, and Lei Zhang. DAB-DETR: Dynamic anchor boxes are better queries for DETR. In *International Conference on Learning Representations*, 2022. 2, 3, 5, 13

[32] Ze Liu, Yutong Lin, Yue Cao, Han Hu, Yixuan Wei, Zheng Zhang, Stephen Lin, and Baining Guo. Swin transformer: Hierarchical vision transformer using shifted windows. *arXiv preprint arXiv:2103.14030*, 2021. 5, 6

[33] Depu Meng, Xiaokang Chen, Zejia Fan, Gang Zeng, Houqiang Li, Yuhui Yuan, Lei Sun, and Jingdong Wang. Conditional detr for fast training convergence. *arXiv preprint arXiv:2108.06152*, 2021. 3, 5

[34] Peihai Miao, Wei Su, Lian Wang, Yongjian Fu, and Xi Li. Referring expression comprehension via cross-level multi-modal fusion. *ArXiv*, abs/2204.09957, 2022. 3

[35] Matthias Minderer, Alexey Gritsenko, Austin Stone, Maxim Neumann, Dirk Weissenborn, Alexey Dosovitskiy, Aravindh Mahendran, Anurag Arnab, Mostafa Dehghani, Zhuoran Shen, Xiao Wang, Xiaohua Zhai, Thomas Kipf, and Neil Houlsby. Simple open-vocabulary object detection with vision transformers. 2022. 4, 5, 8

[36] Vicente Ordonez, Girish Kulkarni, and Tamara L. Berg. Im2text: Describing images using 1 million captioned photographs. *neural information processing systems*, 2011. 8

[37] Bryan A. Plummer, Liwei Wang, Chris M. Cervantes, Juan C. Caicedo, Julia Hockenmaier, and Svetlana Lazebnik. Flickr30k entities: Collecting region-to-phrase correspondences for richer image-to-sentence models. In *Proceedings of the IEEE international conference on computer vision*, pages 2641–2649, 2015. 12

[38] Bryan A. Plummer, Liwei Wang, Christopher M. Cervantes, Juan C. Caicedo, Julia Hockenmaier, and Svetlana Lazebnik. Flickr30k entities: Collecting region-to-phrase correspondences for richer image-to-sentence models. *International Journal of Computer Vision*, 2015. 12

[39] Shaoqing Ren, Kaiming He, Ross Girshick, and Jian Sun. Faster R-CNN: Towards real-time object detection with region proposal networks. In C. Cortes, N. Lawrence, D. Lee, M. Sugiyama, and R. Garnett, editors, *Advances in Neural Information Processing Systems (NeurIPS)*, volume 28. Curran Associates, Inc., 2015. 4

[40] Shaoqing Ren, Kaiming He, Ross Girshick, and Jian Sun. Faster r-cnn: Towards real-time object detection with region

proposal networks. *IEEE Transactions on Pattern Analysis and Machine Intelligence*, 39(6):1137–1149, 2017. 13

[41] Hamid Rezatofighi, Nathan Tsoi, JunYoung Gwak, Amir Sadeghian, Ian Reid, and Silvio Savarese. Generalized intersection over union: A metric and a loss for bounding box regression. In *Proceedings of the IEEE/CVF Conference on Computer Vision and Pattern Recognition*, pages 658–666, 2019. 5, 12

[42] Robin Rombach, Andreas Blattmann, Dominik Lorenz, Patrick Esser, and Björn Ommer. High-resolution image synthesis with latent diffusion models, 2021. 1, 13

[43] Rico Sennrich, Barry Haddow, and Alexandra Birch. Neural machine translation of rare words with subword units. *meeting of the association for computational linguistics*, 2015. 11

[44] Shuai Shao, Zeming Li, Tianyuan Zhang, Chao Peng, Gang Yu, Xiangyu Zhang, Jing Li, and Jian Sun. Objects365: A large-scale, high-quality dataset for object detection. In *Proceedings of the IEEE international conference on computer vision*, pages 8430–8439, 2019. 6, 12

[45] Piyush Sharma, Nan Ding, Sebastian Goodman, and Radu Soricut. Conceptual captions: A cleaned, hypernymed, image alt-text dataset for automatic image captioning. *meeting of the association for computational linguistics*, 2018. 8

[46] Liu Shilong, Liang Yaoyuan, Huang Shijia, Li Feng, Zhang Hao, Su Hang, Zhu Jun, and Zhang Lei. DQ-DETR: Dual query detection transformer for phrase extraction and grounding. In *Proceedings of the AAAI Conference on Artificial Intelligence*, 2023. 4, 8

[47] Peize Sun, Rufeng Zhang, Yi Jiang, Tao Kong, Chenfeng Xu, Wei Zhan, Masayoshi Tomizuka, Lei Li, Zehuan Yuan, Changhu Wang, and Ping Luo. Sparse r-cnn: End-to-end object detection with learnable proposals. In *Proceedings of the IEEE/CVF Conference on Computer Vision and Pattern Recognition*, pages 14454–14463, 2021. 4

[48] Mingxing Tan and Quoc V. Le. Efficientnet: Rethinking model scaling for convolutional neural networks. *international conference on machine learning*, 2019. 8

[49] Bart Thomee, David A. Shamma, Gerald Friedland, Benjamin Elizalde, Karl Ni, Douglas N. Poland, Damian Borth, and Li-Jia Li. Yfcc100m: the new data in multimedia research. *Communications of The ACM*, 2016. 8

[50] Yingming Wang, Xiangyu Zhang, Tong Yang, and Jian Sun. Anchor detr: Query design for transformer-based detector. *national conference on artificial intelligence*, 2021. 3

[51] Thomas Wolf, Lysandre Debut, Victor Sanh, Julien Chaudmont, Clement Delangue, Anthony Moi, Pierrick Cistac, Tim Rault, Rémi Louf, Morgan Funtowicz, et al. Huggingface’s transformers: State-of-the-art natural language processing. *arXiv preprint arXiv:1910.03771*, 2019. 6

[52] Mengde Xu, Zheng Zhang, Han Hu, Jianfeng Wang, Lijuan Wang, Fangyun Wei, Xiang Bai, and Zicheng Liu. End-to-end semi-supervised object detection with soft teacher. *arXiv preprint arXiv:2106.09018*, 2021. 7

[53] Lewei Yao, Jianhua Han, Youpeng Wen, Xiaodan Liang, Dan Xu, Wei Zhang, Zhenguo Li, Chunjing Xu, and Hang Xu. Detclip: Dictionary-enriched visual-concept paralleled pre-training for open-world detection. 2022. 3, 4, 5, 8, 9, 12

[54] Licheng Yu, Zhe Lin, Xiaohui Shen, Jimei Yang, Xin Lu, Mohit Bansal, and Tamara L. Berg. Mattnet: Modular attention network for referring expression comprehension. *computer vision and pattern recognition*, 2018. 8

[55] Lu Yuan, Dongdong Chen, Yi-Ling Chen, Noel Codella, Xiyang Dai, Jianfeng Gao, Houdong Hu, Xuedong Huang, Boxin Li, Chunyuan Li, Ce Liu, Mengchen Liu, Zicheng Liu, Yumao Lu, Yu Shi, Lijuan Wang, Jianfeng Wang, Bin Xiao, Zhen Xiao, Jianwei Yang, Michael Zeng, Luwei Zhou, and Pengchuan Zhang. Florence: A new foundation model for computer vision. 2022. 6, 8

[56] Yuhang Zang, Wei Li, Kaiyang Zhou, Chen Huang, and Chen Change Loy. Open-vocabulary detr with conditional matching. 2022. 2, 4

[57] Alireza Zareian, Kevin Dela Rosa, Derek Hao Hu, and Shih-Fu Chang. Open-vocabulary object detection using captions. In *Proceedings of the IEEE/CVF Conference on Computer Vision and Pattern Recognition*, pages 14393–14402, 2021. 3

[58] Hao Zhang, Feng Li, Shilong Liu, Lei Zhang, Hang Su, Jun Zhu, Lionel M. Ni, and Heung-Yeung Shum. Dino: Detr with improved denoising anchor boxes for end-to-end object detection, 2022. 2, 3, 4, 5, 7, 8, 13

[59] Haotian Zhang, Pengchuan Zhang, Xiaowei Hu, Yen-Chun Chen, Liunian Harold Li, Xiyang Dai, Lijuan Wang, Lu Yuan, Jenq-Neng Hwang, and Jianfeng Gao. Glipv2: Unifying localization and vision-language understanding. 2022. 4, 6, 8

[60] Shifeng Zhang, Cheng Chi, Yongqiang Yao, Zhen Lei, and Stan Z. Li. Bridging the gap between anchor-based and anchor-free detection via adaptive training sample selection. *computer vision and pattern recognition*, 2019. 4

[61] Tiancheng Zhao, Peng Liu, Xiaopeng Lu, and Kyusong Lee. Omdet: Language-aware object detection with large-scale vision-language multi-dataset pre-training. 2022. 4, 8, 9

[62] Yiwu Zhong, Jianwei Yang, Pengchuan Zhang, Chunyuan Li, Noel Codella, Liunian Harold Li, Luwei Zhou, Xiyang Dai, Lu Yuan, Yin Li, and Jianfeng Gao. Regionclip: Region-based language-image pretraining. 2022. 4

[63] Xingyi Zhou, Dequan Wang, and Philipp Krähenbühl. Objects as points. *arXiv preprint arXiv:1904.07850*, 2019. 8

[64] Xizhou Zhu, Weijie Su, Lewei Lu, Bin Li, Xiaogang Wang, and Jifeng Dai. Deformable detr: Deformable transformers for end-to-end object detection. In *ICLR 2021: The Ninth International Conference on Learning Representations*, 2021. 3, 4, 5, 11, 13

A. More Implementation Details

By default, we use 900 queries in our model following DINO. We set the maximum text token number as 256. Using BERT as our text encoder, we follow BERT to tokenize texts with a BPE scheme [43]. We use six feature enhancer layers in the feature enhancer module. The cross-modality decoder is composed of six decoder layers as well. We leverage deformable attention [64] in image cross-attention layers.

Both matching costs and final losses include classification losses (or contrastive losses), box L1 losses, and GIOU [41] losses. Following DINO, we set the weight of classification costs, box L1 costs, and GIOU costs as 2.0, 5.0, and 2.0, respectively, during Hungarian matching. The corresponding loss weights are 1.0, 5.0, and 2.0 in the final loss calculation.

Our Swin Transformer Tiny models are trained on 16 Nvidia V100 GPUs with a total batch size of 32. We extract three image feature scales, from $8\times$ to $32\times$. It is named “4scale” in DINO since we downsample the $32\times$ feature map to $64\times$ as an extra feature scale. For the model with Swin Transformer Large, we extract four image feature scales from backbones, from $4\times$ to $32\times$. The model is trained on 64 Nvidia A100 GPUs with a total batch size of 64.

Item	Value
optimizer	AdamW
lr	1e-4
lr of image backbone	1e-5
lr of text backbone	1e-5
weight decay	0.0001
clip max norm	0.1
number of encoder layers	6
number of decoder layers	6
dim feedforward	2048
hidden dim	256
dropout	0.0
nheads	8
number of queries	900
set cost class	1.0
set cost bbox	5.0
set cost giou	2.0
ce loss coef	2.0
bbox loss coef	5.0
giou loss coef	2.0

Table 8. Hyper-parameters used in our pre-trained models.

B. Data Usage

We use three types of data in our model pre-train.

1. **Detection data.** Following GLIP [26], we reformulate the object detection task to a phrase grounding task by concatenating the category names into text prompts. We use COCO [29], O365 [44], and OpenImage(OI) [19] for our model pretrain. To simulate different text inputs, we randomly sampled category names from all categories in a dataset on the fly during training.
2. **Grounding data.** We use the GoldG and RefC data as grounding data. Both GoldG and RefC are prepro-

cessed by MDETR [18]. These data can be fed into Grounding DINO directly. GoldG contains images in Flickr30k entities [37, 38] and Visual Genome [20]. RefC contains images in RefCOCO, RefCOCO+, and RefCOCOg.

3. **Caption data.** To enhance the model performance on novel categories, we feed the semantic-rich caption data to our model. Following GLIP, we use the pseudo-labeled caption data for model training. A well-trained model generates the pseudo labels.

There are two versions of the O365 dataset, which we termed O365v1 and O365v2, respectively. O365v1 is a subset of O365v2. O365v1 contains about 600K images, while O365v2 contains about 1.7M images. Following previous works [26, 53], we pre-train the Grounding-DINO-T on O365v1 for a fair comparison. The Grounding-DINO-L is pre-trained on O365v2 for a better result.

C. More Results on COCO Detection Benchmarks

C.1. COCO Detection Results under the $1\times$ Setting

We present the performance of Grounding DINO on standard COCO detection benchmark in Table 9. All models are trained with a ResNet-50 [16] backbone for 12 epochs. Grounding DINO achieves 48.1 AP under the research setting, which shows that Grounding DINO is a strong closed-set detector. However, it is inferior compared with the original DINO. We suspect that the new components may make the model harder to optimize than DINO.

D. Detailed Results on ODinW

We present detailed results of Grounding DINO on ODinW35 in Table 10, Table 11, and Table 12.

E. Comparison between DINO and Grounding DINO

To illustrate the difference between DINO and Grounding DINO, we compare DINO and Grounding DINO in Fig. 6. We mark the DINO blocks in gray, while the newly proposed modules are shaded in blue.

F. Visualizations

We present some visualizations in Fig. 7. Our model presents great generalization on different scenes and text inputs. For example, Grounding DINO accurately locates `man in blue` and `child in red` in the last image.

Model	Epochs	AP	AP ₅₀	AP ₇₅	AP _S	AP _M	AP _L
Faster-RCNN(5scale) [40]	12	37.9	58.8	41.1	22.4	41.1	49.1
DETR(DC5) [2]	12	15.5	29.4	14.5	4.3	15.1	26.7
Deformable DETR(4scale) [64]	12	41.1	—	—	—	—	—
DAB-DETR(DC5) [†] [31]	12	38.0	60.3	39.8	19.2	40.9	55.4
Dynamic DETR(5scale) [6]	12	42.9	61.0	46.3	24.6	44.9	54.4
Dynamic Head(5scale) [5]	12	43.0	60.7	46.8	24.7	46.4	53.9
HTC(5scale) [3]	12	42.3	—	—	—	—	—
DN-Deformable-DETR(4scale) [24]	12	43.4	61.9	47.2	24.8	46.8	59.4
DINO-4scale [58]	12	49.0	66.6	53.5	32.0	52.3	63.0
Grounding DINO (4scale)	12	48.1	65.8	52.3	30.4	51.3	62.3

Table 9. Results for Grounding DINO and other detection models with the ResNet50 backbone on COCO val2017 trained with 12 epochs (the so called 1× setting).

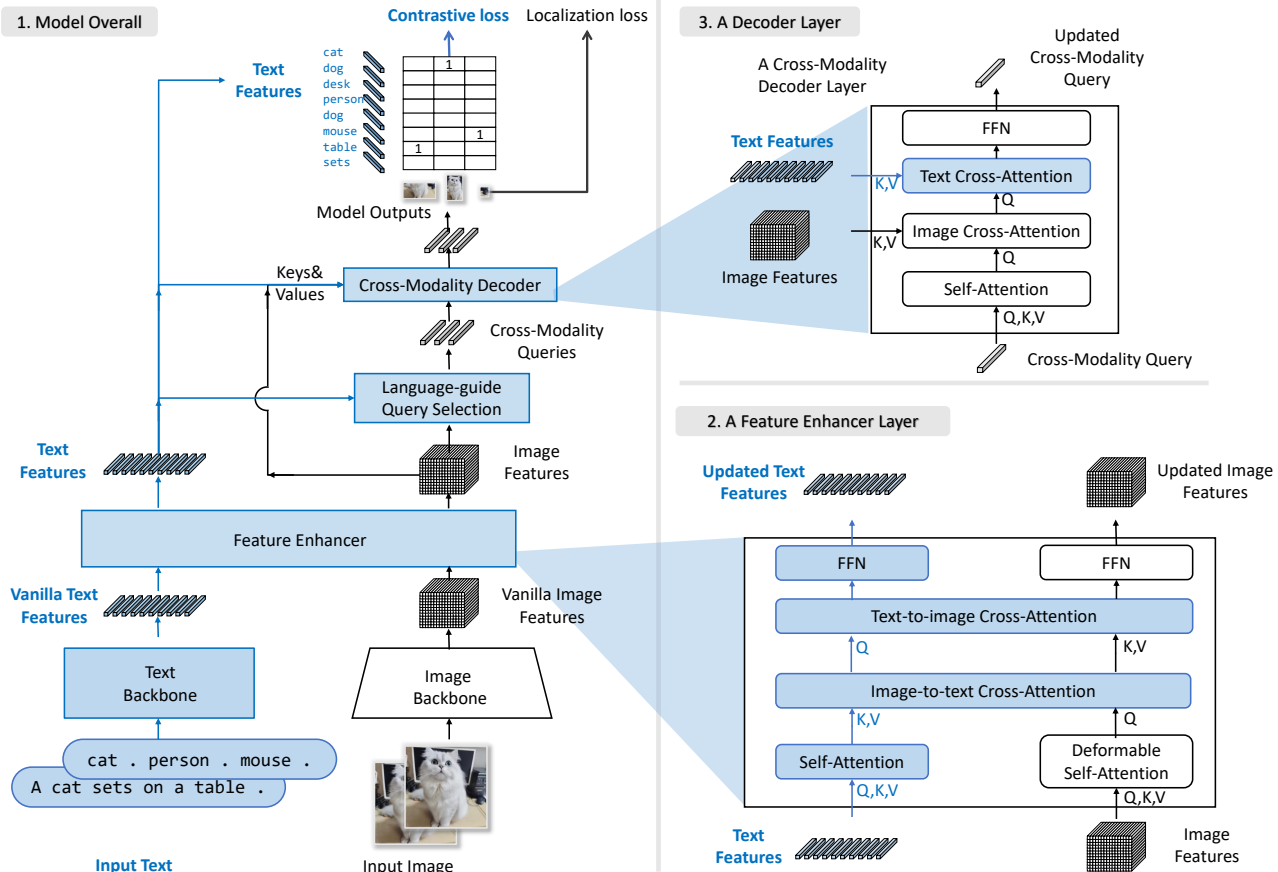


Figure 6. Comparison between DINO and our Grounding DINO. We mark the modifications in blue. Best view in color.

G. Marry Grounding DINO with Stable Diffusion

Grounding DINO L finishes the detection task in Fig. 1. The results in Fig. 1 (b) are generated by two processes. First, we detect objects with Grounding DINO.

Then we generate masks by masking out the detected objects or backgrounds. After that, we feed original images, image masks, and generation prompts to the stable diffusion models [42] to render new images. We use the releases checkpoints in <https://github.com/Stability-AI/stablediffusion> for new image generation. More re-



Figure 7. Visualizations of model outputs.

Dataset	AP	AP ₅₀	AP ₇₅	AP _S	AP _M	AP _L
AerialMaritimeDrone.large	9.48	15.61	8.35	8.72	10.28	2.91
AerialMaritimeDrone.tiled	17.56	26.35	13.89	0	1.61	28.7
AmericanSignLanguageLetters	1.45	2.21	1.39	-1	-1	1.81
Aquarium	18.83	34.32	18.19	10.65	20.64	21.52
BCCD.BCCD	6.17	11.31	6.04	1.27	9.09	6.89
ChessPiece	6.99	11.13	9.03	-1	-1	8.11
CottontailRabbits	71.93	85.05	85.05	-1	70	73.58
DroneControl.Drone_Control	6.15	10.95	6.23	2.08	6.91	6.16
EgoHands.generic	48.07	75.06	56.52	1.48	11.42	51.84
EgoHands.specific	0.66	1.25	0.64	0	0.02	0.92
HardHatWorkers	2.39	9.17	1.07	2.13	4.32	4.6
MaskWearing	0.58	1.43	0.56	0.12	0.51	4.66
MountainDewCommercial	18.22	29.73	21.33	0	23.23	49.8
NorthAmericaMushrooms	65.48	71.26	66.18	-1	-1	65.49
OxfordPets.by-breed	0.27	0.6	0.21	-1	1.38	0.33
OxfordPets.by-species	1.66	5.02	1	-1	0.65	1.89
PKLot.640	0.08	0.26	0.02	0.14	0.79	0.11
Packages	56.34	68.65	68.65	-1	-1	56.34
PascalVOC	47.21	57.59	51.28	16.53	39.51	58.5
Raccoon.Raccoon	44.82	76.44	46.16	-1	17.08	48.56
ShellfishOpenImages	23.08	32.21	26.94	-1	18.82	23.28
ThermalCheetah	12.9	19.65	14.72	0	8.35	50.15
UnoCards	0.87	1.52	0.96	2.91	2.18	-1
VehiclesOpenImages	59.24	71.88	64.69	7.42	32.38	72.21
WildfireSmoke	25.6	43.96	25.34	5.03	18.85	42.59
oggleBoards	0.81	2.92	0.12	2.96	1.13	-1
brackishUnderwater	1.3	1.88	1.4	0.99	1.75	11.39
dice.mediumColor	0.16	0.72	0.07	0.38	3.3	2.23
openPoetryVision	0.18	0.5	0.06	-1	0.25	0.17
pistols	46.4	66.47	47.98	4.51	22.94	55.03
plantdoc	0.34	0.51	0.35	-1	0.28	0.86
pothole	19.87	28.94	22.23	12.49	15.6	28.78
selfdrivingCa	9.46	19.13	8.19	0.85	6.82	16.51
thermalDogsAndPeople	72.67	86.65	79.98	33.93	30.2	86.71
websiteScreenshots	1.51	2.8	1.42	0.85	2.06	2.59

Table 10. Detailed results on 35 datasets in ODinW of Grounding DINO with Swin-T pre-trained on O365 and GoldG.

sults are available in Figure 8.

Using GLIGEN for Grounded Generation To enable fine-grained image editing, we combine the Grounding DINO with GLIGEN [?]. GLIGEN supports grounding results as inputs and can generate objects on specific positions. We can assign each bounding box an object with GLIGEN, as the cake and dog in Figure 9 (c) (d). Moreover, GLIGEN can full fill each bounding box, which results in better visualization, as that in Figure 9 (a) (b). For example,

Dataset	AP	AP ₅₀	AP ₇₅	AP _S	AP _M	AP _L
AerialMaritimeDrone.large	10.3	18.17	9.21	8.92	11.2	7.35
AerialMaritimeDrone.tiled	17.5	28.04	18.58	0	3.64	24.16
AmericanSignLanguageLetters	0.78	1.17	0.76	-1	-1	1.02
Aquarium	18.64	35.27	17.29	11.33	17.8	21.34
BCCD.BCCD	11.96	22.77	8.65	0.16	5.02	13.15
ChessPiece	15.62	22.02	20.19	-1	-1	15.72
CottontailRabbits	67.61	78.82	78.82	-1	70	68.09
DroneControl.Drone_Control	4.99	8.76	5	0.65	5.03	8.61
EgoHands.generic	57.64	90.18	66.78	3.74	24.67	61.33
EgoHands.specific	0.69	1.37	0.63	0	0.02	1.03
HardHatWorkers	4.05	13.16	1.96	2.29	7.55	9.81
MaskWearing	0.25	0.81	0.15	0.09	0.13	2.78
MountainDewCommercial	25.46	39.08	28.89	0	32.53	58.38
NorthAmericaMushrooms	68.18	72.89	69.75	-1	-1	68.62
OxfordPets.by-breed	0.21	0.42	0.22	-1	2.91	0.17
OxfordPets.by-species	1.3	3.95	0.71	-1	0.28	1.62
PKLot.640	0.06	0.18	0.02	0.03	0.59	0.15
Packages	60.53	76.24	76.24	-1	-1	60.53
PascalVOC	55.65	66.51	60.47	19.61	44.25	67.21
Raccoon.Raccoon	60.07	84.81	66.5	-1	11.23	65.86
ShellfishOpenImages	29.56	38.08	33.5	-1	6.38	29.95
ThermalCheetah	17.72	25.93	19.61	1.04	20.02	63.69
UnoCards	0.81	1.3	1	2.6	1.01	-1
VehiclesOpenImages	58.49	71.56	63.64	8.22	28.03	71.1
WildfireSmoke	20.04	39.74	22.49	4.13	15.71	30.41
oggleBoards	0.29	1.15	0.04	1.8	0.57	-1
brackishUnderwater	1.47	2.34	1.58	2.32	3.31	9.96
dice.mediumColor	0.33	1.38	0.15	0.03	1.05	12.57
openPoetryVision	0.05	0.19	0	-1	0.09	0.21
pistols	66.99	86.34	72.65	16.25	39.24	75.98
plantdoc	0.36	0.47	0.39	-1	0.24	0.82
pothole	25.21	38.21	26.01	8.94	18.45	39.28
selfdrivingCa	9.95	20.55	8.28	1.36	7.27	15.46
thermalDogsAndPeople	67.89	80.85	78.66	45.05	30.24	85.56
websiteScreenshots	1.3	2.26	1.21	0.95	1.81	2.23

Table 11. Detailed results on 35 datasets in ODinW of Grounding DINO with Swin-T pre-trained on O365, GoldG, and Cap4M.

we use the same generative prompt in Figure 8 (b) and Figure 9 (b). The GLIGEN results ensure each bounding box with an object and fulfills the detected regions.

H. Effects of RefC and COCO Data

We add the RefCOCO/+g (we note it as ‘‘RefC’’ in tables) and COCO into training in some settings. We explore the influence of these data in Table 13. The results show that RefC helps improve the COCO zero-shot and fine-tuning performance but hurts the LVIS and ODinW results. With

Figure 8. Combination of Grounding DINO and Stable Diffusion. We first detect objects with Grounding DINO and then perform image inpainting with Stable Diffusion. * The input human face in the row (e) is generated by StyleGAN.

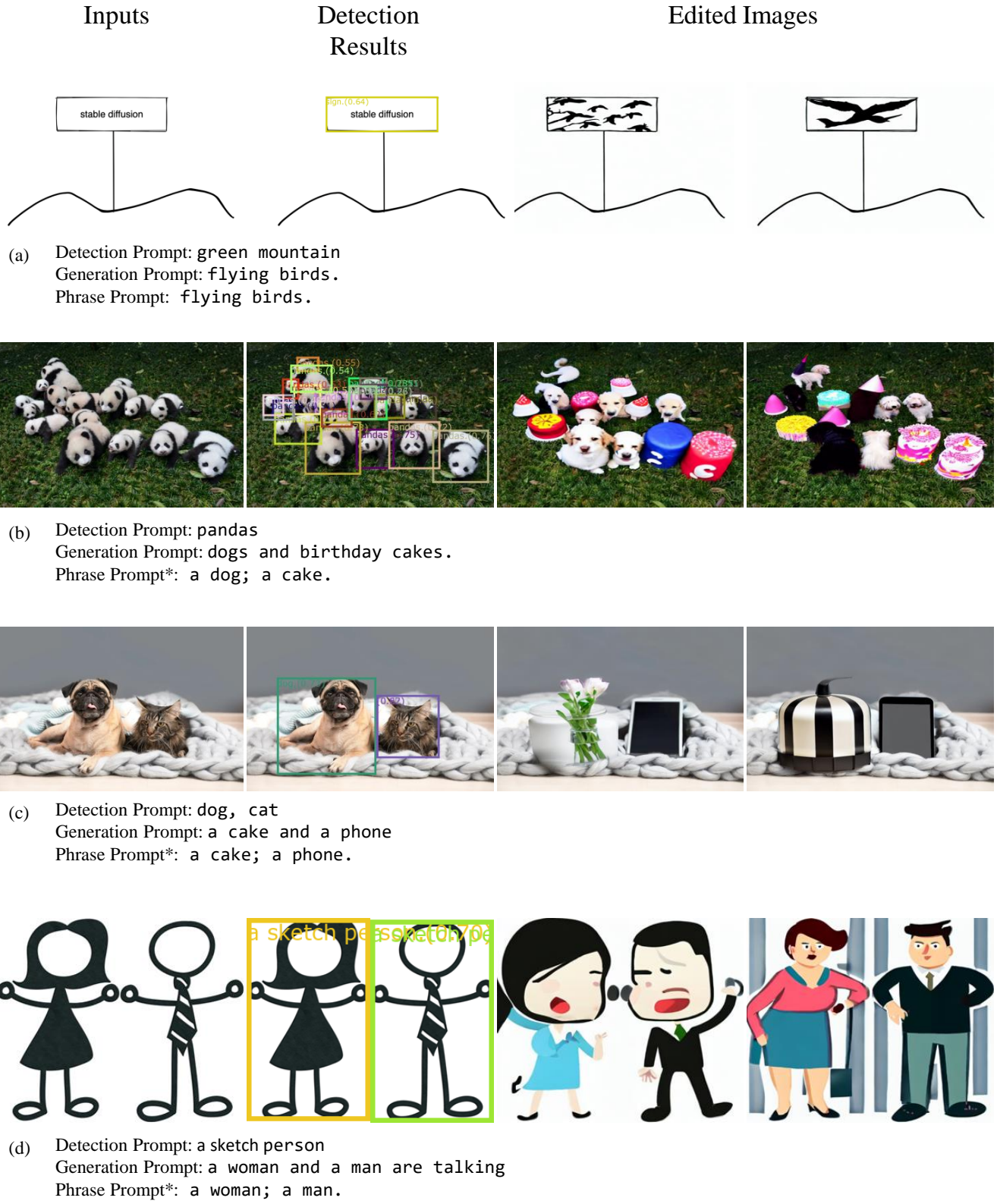


Figure 9. Combination of Grounding DINO and GLIGEN. We first detect objects with Grounding DINO and then perform image inpainting with GLIGEN. * The phrase prompts are separated by semicolons. We assign phrase prompts to bounding boxes randomly.

Dataset	AP	AP ₅₀	AP ₇₅	AP _S	AP _M	AP _L
AerialMaritimeDrone.large	12.64	18.44	14.75	9.15	19.16	0.98
AerialMaritimeDrone.tiled	20.47	34.81	12.79	0	7.61	26.93
AmericanSignLanguageLetters	3.94	4.84	4	-1	-1	4.48
Aquarium	28.14	45.47	30.97	12.1	24.71	39.42
BCCD.BCCD	23.85	36.92	28.88	0.3	10.8	24.43
ChessPiece	18.44	26.3	23.33	-1	-1	18.62
CottontailRabbits	71.66	88.48	88.48	-1	66	73.04
DroneControl.Drone_Control	7.16	11.56	7.67	2.29	10.6	7.68
EgoHands.generic	52.08	81.57	59.15	1.12	31.78	55.46
EgoHands.specific	1.22	2.28	1.2	0	0.05	1.5
HardHatWorkers	9.14	23.64	5.6	5.09	15.34	13.59
MaskWearing	1.64	4.69	1.18	0.44	1.05	8.67
MountainDewCommercial	33.28	53.59	32.76	0	35.86	80
NorthAmericaMushrooms	72.33	73.18	73.18	-1	-1	72.39
OxfordPets.by-breed	0.58	1.05	0.59	-1	4.46	0.6
OxfordPets.by-species	1.64	4.8	0.87	-1	1.51	1.8
PKLot.640	0.25	0.71	0.05	0.31	1.44	0.4
Packages	63.86	76.24	76.24	-1	-1	63.86
PascalVOC	66.01	76.65	71.8	32.01	55.7	75.37
Raccoon.Raccoon	65.81	90.39	69.93	-1	26	68.97
ShellfishOpenImages	62.47	74.25	70.07	-1	26	63.06
ThermalCheetah	21.33	26.11	24.92	2.39	15.84	75.34
UnoCards	0.52	0.84	0.66	3.02	0.92	-1
VehiclesOpenImages	62.74	75.15	67.23	10.66	47.46	76.36
WildfireSmoke	23.66	45.72	25.06	1.58	22.22	35.27
oggleBoards	0.28	1.04	0.05	5.64	0.7	-1
brackishUnderwater	2.41	3.39	2.79	4.43	3.88	21.22
dice.mediumColor	0.26	1.15	0.03	0	1.09	4.07
openPoetryVision	0.08	0.35	0.01	-1	0.15	0.11
pistols	71.4	90.69	77.21	18.74	39.58	80.78
plantdoc	2.02	2.64	2.37	-1	0.5	2.82
pothole	30.4	44.22	33.84	12.27	18.84	48.57
selfdrivingCa	9.25	17.72	8.39	1.93	7.03	13.02
thermalDogsAndPeople	72.02	86.02	79.47	29.16	68.05	86.75
websiteScreenshots	1.32	2.64	1.16	0.79	1.8	2.46

Table 12. Detailed results on 35 datasets in ODinW of Grounding DINO with Swin-L pre-trained on O365, OI, GoldG, Cap4M, COCO, and RefC.

Model	Pre-Train	COCO minival		LVIS minival Zero-Shot	ODinW Zero-Shot
		Zero-Shot	Fine-Tune		
Grounding DINO T	O365,GoldG	48.1	57.1	25.6	20.0
Grounding DINO T	O365,GoldG,RefC	48.5	57.3	21.9	17.7
Grounding DINO T	O365,GoldG,RefC,COCO	56.1	57.5	22.3	17.4

Table 13. Impacts of RefC and COCO data for open-set settings. All models are trained with a Swin Transformer Tiny backbone.

COCO introduced, the COCO results is greatly improved. It shows that COCO brings marginal improvements on LVIS and slightly decreases on ODinW.

Model	params	GFLOPS	FPS
GLIP-T [26]	232M	488G	6.11
Grounding DINO T (Ours)	172M	464G	8.37

Table 14. Comparison of model size and model efficiency between GLIP and Grounding DINO.

I. Model Efficiency

We compare the model size and efficiency between Grounding-DINO-T and GLIP-T in Table 14. The results show that our model has a smaller parameter size and better efficiency than GLIP.